NLR TECHNICAL PUBLICATION

TP 97036 U

DERIVATION OF LATERAL AND VERTICAL GUST STATISTICS FROM IN-FLIGHT MEASUREMENTS

by

P.A. van Gelder

This paper has been prepared for presentation at the 38th AIAA/ASME/ASCE/AHS/ASC Structures, Structural Dynamics and Materials Conference, April 7-10, 1997, Kissimmee, Florida.

Division : Structures and Materials
Prepared : PAvG/ 17/2
Approved : JBdJ/ 18/2

Completed : 970121
Order number : 541.201
Typ. : MM

Contents

Abstract 5

Introduction 5

Measurements 5

Gust Analysis 6
- Discrete vertical gust 6
- Continuous vertical gust 8
- Estimation of PSD-gust parameters (P's and b's) 10
- Discrete lateral gust 12
- Continuous lateral gust 12

Conclusions 13

Acknowledgement 14

References 14

Abbreviations 14

2 Tables
10 Figures

(14 pages in total)

This page is intentionally left blank.

DERIVATION OF LATERAL AND VERTICAL GUST STATISTICS FROM IN-FLIGHT MEASUREMENTS

P.A. van Gelder
National Aerospace Laboratory NLR
Anthony Fokkerweg 2
NL-1059 CM Amsterdam, The Netherlands

Abstract

An in-flight tail load measurement program has been carried out in The Netherlands in order to validate the procedures that are currently used for the determination of tail load spectra and to improve the statistical knowledge of gusts and manoeuvres, with respect to tail loads.
In this measurement program tail loads, including lateral accelerations of the rear fuselage and vertical centre of gravity accelerations, have been obtained from a commercially operated Fokker 100 aircraft flying European routes.

The paper describes how the vertical and lateral gust statistics have been derived from measured accelerations.
A comparison is made between vertical and lateral gust statistics, both for discrete and continuous types of gusts.

Vertical gust statistics (discrete and PSD) compared very well with earlier results from FAA/NLR. Also the continuous (PSD) gust statistics for lateral gusts compared very well with the results found for vertical gusts.
The derived lateral (discrete) gust velocities however produced results that are not in line with the vertical gust velocities, indicating that care should be taken with the application of the discrete lateral gust approach.

Introduction

According to current requirements from the Federal Aviation Administration (FAR-25) and Joint Airworthiness Authorities (JAR-25) aircraft design loads due to gust and turbulence need to be determined for (tuned) discrete gusts with a prescribed shape (one-minus-cosine) and for continuous turbulence with a prescribed power spectral density (PSD) function (Von Karman).
Gust design speeds are prescribed for discrete gust and continuous turbulence and vary with altitude and design condition (V_B, V_C, etc.).

In-flight measurements on routinely operated commercial flights have been carried out in the past[1-5] and are being carried out at the moment for instance by a program sponsored by the FAA[11,12] from which vertical gust velocities can be derived and can be used to substantiate the current requirements.
For lateral gust no such data is available and at the moment it is assumed that gust characteristics for vertical and lateral directions are comparable.
The current paper describes the derivation of both vertical and lateral gust statistics from the recordings of more than 2000 flights of a commercially operated civil transport aircraft.

Measurements

An in-flight measurement program has been carried out in The Netherlands in order to validate the procedures that are currently used for the determination of tail load spectra and to improve the statistical knowledge of gusts and manoeuvres, with respect to tail loads.
In this measurement program tail loads have been obtained from a commercially operated Fokker 100 aircraft (Fig. 1) in service with a Dutch airline company (KLM). Special attention was paid to the measurement set-up, since neither interference with other systems nor adverse effects on the availability of the aircraft were permissible.
These problems were solved by using a combined system for the recording of data. A relevant number of aircraft parameters, including vertical cg-accelerations, recorded by the existing Aircraft Condition Monitoring System (ACMS), were combined with loads parameters recorded by a stand-alone dedicated data recorder. This data recorder was operated without any interference to other aircraft systems. The tailplane was instrumented with a number of calibrated strain gauges in order to measure the bending moment of one stabilizer half, and its symmetrical and anti-symmetrical component. Also lateral accelerations of the rear fuselage were measured in order to study the correlation of the anti-symmetric tailplane bending moments with lateral accelerations of the rear fuselage and also for the derivation of lateral gust statistics.

More details on the instrumentation, calibration, data-recording and data-base generation can be found in references 8-10.

Fig. 1 Fokker 100 tail structure

Gust Analysis

For the derivation of gust statistics from the recorded acceleration data two methods will be used. One method is based on the discrete gust, the other on the continuous gust concept. Both methods will be applied to derive vertical and lateral gust statistics. The methods are extensively described in reference 6 for application to vertical gust and have been applied to a couple of European databases[7].
In this paper special attention will be given to the derivation of lateral gust statistics.

Table 1 Altitude bands for gust statistics

Band			Altitude (ft)
1		<	1500
2	1500	-	4500
3	4500	-	9500
4	9500	-	14500
5	14500	-	19500
6	19500	-	24500
7	24500	-	29500
8	29500	-	34500
9	34500	-	39500
10	39500	>	

The analysis is performed for the same altitude bands as applied by the FAA/NLR report[7]. The altitude bands (see also table 1) have been chosen in such a way that flight levels for higher altitudes (multiples of 1000 ft) fall within these bands.

Discrete vertical gust

In the discrete gust approach the atmospheric turbulence is assumed to consist of separate "discrete" bumps with a specific gust profile and magnitude U. This discrete gust causes the aircraft to respond with a maximum (vertical) acceleration Δn_z. The relation between the incremental load factor (Δn_z) and the gust velocity U is given by:

$$\Delta n_z = \bar{C} * U \qquad (1)$$

where $\bar{C}$ is called the response factor.
This equation can also be used to derive the gust velocity from measured (peak) accelerations, according to:

$$U_{de} = \frac{\Delta n_z}{\bar{C}} \qquad (2)$$

The subscript "de" (derived) is used here to indicate that U is not a truly measured gust velocity but in fact a reduced acceleration value. In this discrete gust approach one peak of acceleration (Δn_z) yields one peak of gust (U_{de}).
In general, the response factor $\bar{C}$ is a function of shape and length of the gust profile and response behaviour of the aircraft.
Pratt and Walker[1] have calculated the response factor $\bar{C}$ with the following assumptions:

1) The gust profile has a "(1 - cosine)" shape with a length of 25 wing chords.
2) The aircraft is assumed to be infinitely stiff and responds only in vertical plunging motions (no pitching).
3) Aerodynamic inertia has been included.

The resulting $\bar{C}$-values found for a number of aircraft can be approximated by the following function:

$$\bar{C} = \frac{\rho_0 V_E C_{L_\alpha} S}{2mg} F(\mu_g) \qquad (3)$$

where $F(\mu_g)$ is the so-called gust alleviation factor, according to:

$$F(\mu_g) = \frac{0.88\,\mu_g}{5.3 + \mu_g}, \quad \mu_g = \frac{2m}{\rho \bar{c} S C_{L_\alpha}} \qquad (4)$$

Equation (3) is known as the "Pratt-formula" and has not only been used for the reduction of the NACA VGH-data, but also in the airworthiness requirements for defining gust design-load factors, not because of the strong physical background, but mainly because of its simplicity.

Derived gust velocities have been calculated for the given altitude bands from the peaks in the vertical acceleration data. These peaks are selected from the measured acceleration data according to the 'peak-between-means' criterion, which means that between two successive crossings of $n_z = 1$ only the highest (positive) peak or lowest (negative) valley is selected, see also reference 7 and the illustration in figure 2.
The parameters of equation (3) are all available from the database except values for C_{L_α}. This parameter is a function of Mach number, altitude and flap position. The parameter values have been derived from tabulated data.

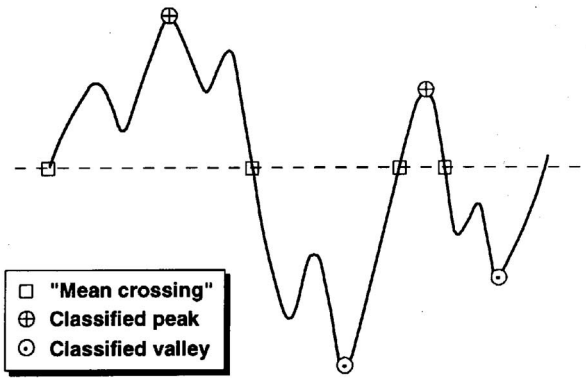

Fig. 2 'Peak-between-means' classification criterion

In order to separate manoeuvre induced accelerations (as good as possible) from the gust induced accelerations a so-called bank-angle correction is applied. This correction to the vertical cg-acceleration (or load factor) is based on the increment in acceleration during (steady) turning manoeuvres[6]:

$$(\Delta n_z)_{gust} = (\Delta n_z) - [1/\cos\phi - 1]$$

where

$(\Delta n_z)_{gust}$ = corrected vertical acceleration
(Δn_z) = measured vertical acceleration
ϕ = bank angle

So in summary the following procedure has been applied:

1. Vertical cg-accelerations per flight are available from the database in the form of a peak-valley sequence.
2. A correction is applied to correct for turning manoeuvres.
3. A peak-between-means selection criterion is applied to the corrected sequence.
4. This corrected acceleration (load factor) sequence is reduced to derived gust velocities.

When it is assumed that upward and downward gusts are equally probable a symmetric acceleration (load factor) spectrum should be found. However when accelerations due to (elevator) manoeuvres are present, they will be mostly positive, which will shift the spectrum in an upward (positive) direction.
From figure 3 it is observed that the bank-angle correction leads to a more 'symmetric' upper and lower half of the spectrum, because the incremental accelerations (load factor) due to turning manoeuvres have been eliminated. This is illustrated by connecting points of equal magnitude but different sign. When roll-correction has been applied these lines tend to 'straighten-up' towards a more vertical situation (vertical corresponds to symmetric).
Corrections for accelerations due to symmetric manoeuvres have not been taken into account, because it is very difficult to distinguish between manoeuvres purely for flight control and manoeuvres to correct for (gust) disturbances.
An improvement of the spectrum at altitudes below 1500 feet could be realised by the elimination of accelerations due to the rotation and flare manoeuvres, during take-off and landing respectively.

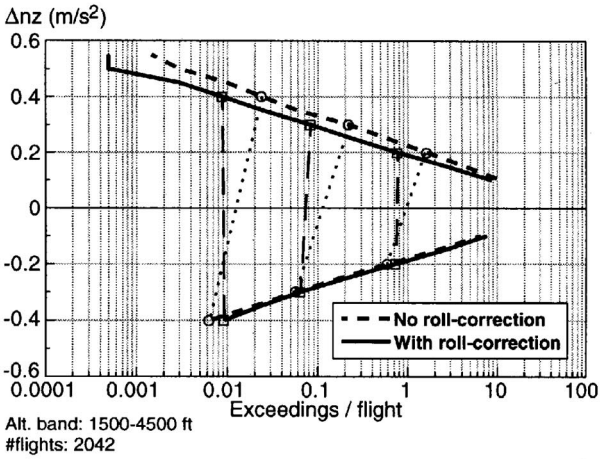

Fig. 3 Effect of bank-angle correction to Δnz

In figures 4a-c the resulting derived vertical gust-velocities for the Fokker 100 database (including roll correction), have been plotted for three altitude bands. In the two lower altitude bands most acceleration (gust) peaks have been encountered (> 60%) while the altitude band between 29500 and 34500 feet is representative for a large part of all distance flown (27 %).

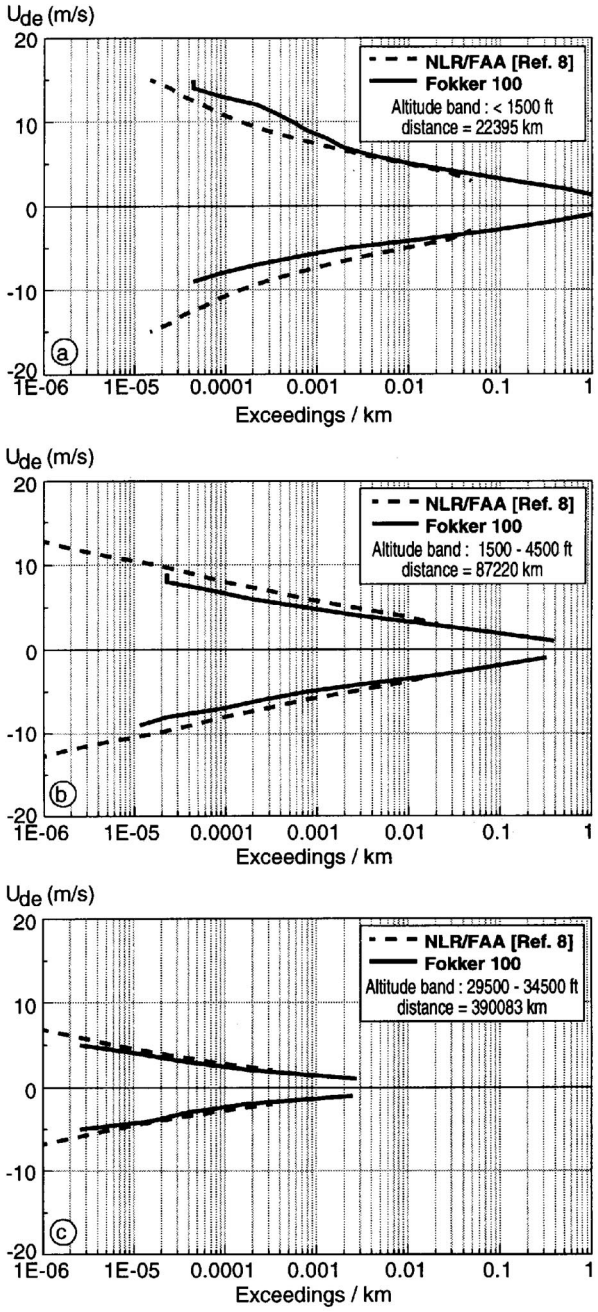

Fig. 4 Comparison of vertical U_{de}'s

The results are presented in combination with the derived gust velocities of the FAA/NLR study[7] which have been obtained from databases of Boeing 747 aircraft (KSSU), the RAE (Fatigue meter) database and the ONERA (CAADRP) database. A summary of these databases with respect to accumulated flights, flown distance and flight hours is given in table 2.

From the derived U_{de}-exceedance curves, the following is concluded:

- For all altitude bands there is a very good agreement especially at altitudes between 24500 - 34500 ft where 43 % of the total flight distance has been flown. For example figure 4c shows the results of altitude band 29500-34500 ft.
- In all cases, except at altitudes below 1500 ft (see figure 4a), the Fokker 100 results indicate equal or less gust-exceedances compared to reference 7.
- At altitudes below 1500 feet the spectrum is very a-symmetric (see figure 4c) which will be mainly caused by pitching manoeuvres during take-off and landing. These manoeuvres cause positive load factor increments which will yield an offset in positive direction of the U_{de}-spectrum.

Table 2 Summary of contents of databases[7,10]

	flights	flight-hrs [hrs]	distance [10^6 km]
ACMS (KSSU / Boeing 747)	24,358	121,893	105
Fatiguemeter data (RAE)	10,697	25,144	12
ONERA (CAADRP / extreme events)	838,657	1,781,548	1,290
Fokker 100	2,063	2,269	1.5

Continuous vertical gust

Different from the deterministic approach that describes atmospheric turbulence as a sequence of discrete bumps (gusts), is the stochastic approach which describes turbulence as a random process. The (linear) incremental cg-acceleration (load factor) response of an aircraft flying through a stationary random gust field with rms value σ_w will also be stationary random, with rms value $\sigma_{\Delta n}$. The ratio $\sigma_{\Delta n}/\sigma_w$ is the response factor $\bar{A}$. $\bar{A}$ is to a large extend equivalent to $\bar{C}$ as described in the previous section. This similarity has led to the "pseudo-discrete" PSD gust velocity U_σ, with:

$$\Delta n_z = \bar{A} * U_\sigma \qquad (6)$$

This formulation is used in current airworthiness requirements (FAR25 & JAR25). $\bar{A}$ is the weighted average response of an aircraft to atmospheric turbulence of which the properties can be described by a spectrum. $\bar{A}$ is calculated by integration over all frequencies of the frequency dependent squared response function times the power spectral density function of the turbulence:

$$\bar{A} = \left[\int_0^\infty |H_{\Delta n,w}(j\omega)|^2 \cdot \Phi_w^n(\omega) \cdot d\omega \right]^{\frac{1}{2}} \qquad (7)$$

The spectrum shape $\Phi_w(\omega)$ for isotropic turbulence, as proposed by Von Karman, and as used in the airworthiness requirements is given by:

$$\Phi_w^n(\omega) = \frac{L}{\pi V} \frac{1+\frac{8}{3}(1.339\omega\frac{L}{V})^2}{\{1+(1.339\omega\frac{L}{V})^2\}^{11/6}} \qquad (8)$$

$\bar{A}$-values for a wide variety of aircraft and aircraft conditions have been calculated by Houbolt[14]. The results could be very well approximated by the simple expression:

$$\bar{A} = \frac{\rho_0 V_E C_{L_\alpha} S}{2 m g} \cdot F(PSD) \qquad (9)$$

where

$$F(PSD) = \frac{11.8}{\sqrt{\pi}} \left(\frac{\bar{c}}{2L}\right)^{\frac{1}{3}} \sqrt{\frac{\mu_g}{110+\mu_g}} \qquad (10)$$

F(PSD) is equivalent to $F(\mu_g)$ from equation (4), however it is not only a function the mass parameter μ_g but also of the scaled gust length.

In the discrete gust concept turbulence is considered to be composed of a discrete number of gusts (bumps) per kilometre flown. Each aircraft flying through this turbulence experiences the same number of gusts (bumps).
The exceedance curve per kilometre for a specific altitude and flight condition reads:

$$N(\Delta n) = B_1 e^{-\frac{\Delta n}{a_1 \bar{c}}} + B_2 e^{-\frac{\Delta n}{a_2 \bar{c}}} \qquad (11)$$

Note: the total number of Δn-peaks per km equals $(B_1 + B_2)$.

In the PSD-concept the number of Δn response peaks depends on aircraft properties and is accounted for by the N(0)-parameter according to:

$$N(\Delta n) = N(0) \left\{ P_1 e^{-\frac{\Delta n}{b_1 \bar{A}}} + P_2 e^{-\frac{\Delta n}{b_2 \bar{A}}} \right\} \qquad (12)$$

Note: the total number of Δn-peaks per km equals $N(0).(P_1 + P_2)$.

In order to account for the variation of N(0) an approximation is given by Houbolt[14]:

$$N(0) = \frac{496}{\pi\bar{c}} \cdot (\mu_g)^{-.46} \quad \text{(per km)} \qquad (13a)$$

or:

$$N(0) = N_0(0) \cdot \left(\frac{\rho}{\rho_0}\right)^{46} \quad \text{(per km)} \qquad (13b)$$

with:

$$N_0(0) = \frac{496}{\pi\bar{c}} \cdot \left(\frac{2m}{S\rho_0 C_{L_\alpha} \bar{c}}\right)^{-.46} \quad \text{(per km)} \qquad (13c)$$

Substituting $U_\sigma = \Delta n_z / \bar{A}$ into equation (12) yields:

$$N(U_\sigma) = N(0) \cdot \left\{ P_1 e^{-\frac{U_\sigma}{b_1}} + P_2 e^{-\frac{U_\sigma}{b_2}} \right\} \qquad (14)$$

This formulation has been applied for the reduction of Δn_z statistics to $N(U_\sigma)$ exceedances.
In order to compare 'physical' results ('real' exceedances rather then non-dimensional exceedances) a reference value $N(0)_{ref}$ is introduced similar to reference 6, such that:

$$\frac{N(U_\sigma)}{N(0)} \cdot N(0)_{ref} = N(0)_{ref} \cdot \left\{ P_1 e^{-\frac{U_\sigma}{b_1}} + P_2 e^{-\frac{U_\sigma}{b_2}} \right\} \qquad (15)$$

This means that one single Δn-peak 'produces' $N(0)_{ref}/N(0)$ occurrences of a gust velocity with magnitude U_σ, which are found from:

$$\frac{N(0)_{ref}}{N(0)} = \frac{N_0(0)_{ref}}{N_0(0)}$$

$$= N_0(0)_{ref} \cdot \frac{\pi\bar{c}}{496} \cdot \left(\frac{2m}{\rho_0 S\bar{c} C_{L_\alpha}}\right)^{+.46}$$

and $N_0(0)_{ref} = 8$ [-/km].

Gust-velocity exceedances have been calculated for the given altitude bands from the peaks in the vertical acceleration data according to the "peak-between-means" criterion similar to the calculation of U_{de} as described in the previous chapter but with the "Houbolt" instead of the "Pratt" formula. Results (including bank-angle correction) for the three most interesting altitude bands, similar to the presentation of the U_{de} results are presented in figures 5a-c in combination with the results from the FAA/NLR study[7].

The results are very similar to the comparison of U_{de} with the FAA/NLR data. Equal or less exceedances for the Fokker 100 in all altitude bands (except below 1500 ft) and a very a-symmetric spectrum at altitudes below 1500 ft, most likely due to pitching manoeuvres.

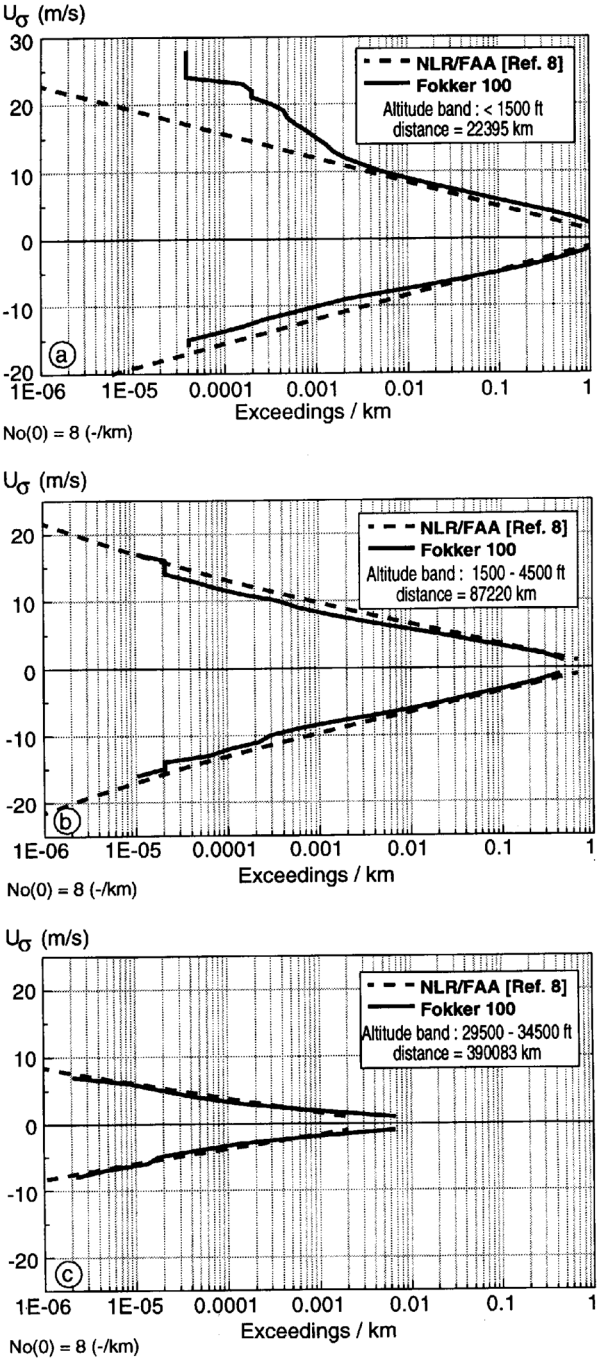

Fig. 5 Comparison of vertical U_σ's

Estimation of PSD-gust parameters (P's and b's)

According to the airworthiness requirements (FAR25, JAR25) the U_σ-exceedance curve is defined as:

$$N(U_\sigma) = N(0).\left\{ P_1 e^{-\frac{U_\sigma}{b_1}} + P_2 e^{-\frac{U_\sigma}{b_2}} \right\} \qquad (16)$$

In this report U_σ-exceedances have been obtained with a reference value similar to references 6 and 7 and consequently must be used here again.

$$N(0)_{ref} = N_0(0)_{ref} \cdot \left(\frac{\rho}{\rho_0}\right)^{0.46} \qquad (17)$$

and

$$N_0(0)_{ref} = 8 \ [km^{-1}]$$

The parameters b1, b2 and P1, P2 have been estimated from the 'one sided' U_σ-curves, found from the geometric mean (logarithmic average) of corresponding upward and downward gust velocities (see also figure 6):

$$N(|U_\sigma|) = \sqrt{N(U_\sigma^+) * N(U_\sigma^-)} = \frac{1}{2}.\left(\ln\{N(U_\sigma^+)\} + \ln\{N(U_\sigma^-)\}\right) \qquad (18)$$

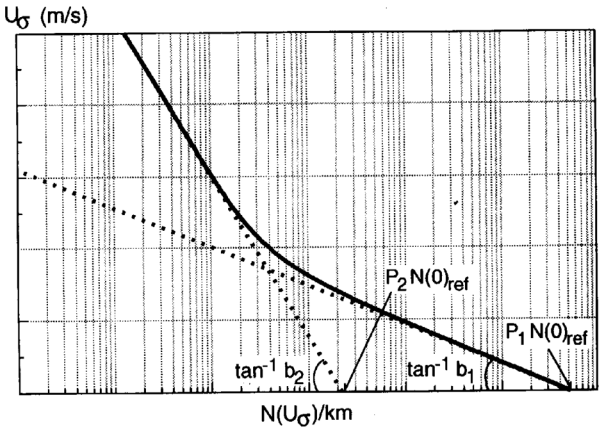

Fig. 6 Approximation of P's and b's

During the ±2000 flights contained within the Fokker 100 database not many 'storm conditions' have been encountered. Therefore it is very difficult to find a good approximation of the 'storm' part of equation 16 (i.e. b_2 and P_2). To find the best approximation a constrained optimization procedure has been used in which the parameter b_2^- (slope of the 'storm' part of the curve) has been fixed to the FAR-value.

Results of the approximation are graphically presented for three altitude bands in figures 7a-c. Some unrealistic points at the upper or lower end of the curves have been given a smaller 'weighting factor' so they would have less influence on the approximation.
The resulting parameters are compared to the FAR/JAR-values and results from reference 7 in figures 8a-b.

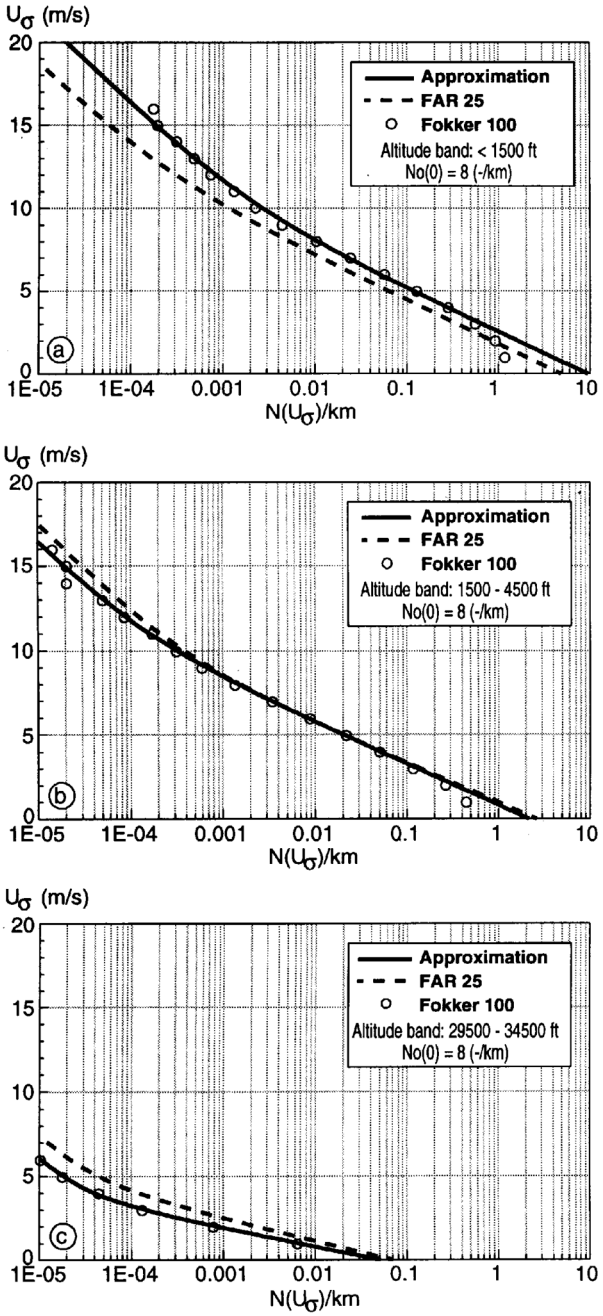

Fig. 7 Approximation of U_σ exceedance curve

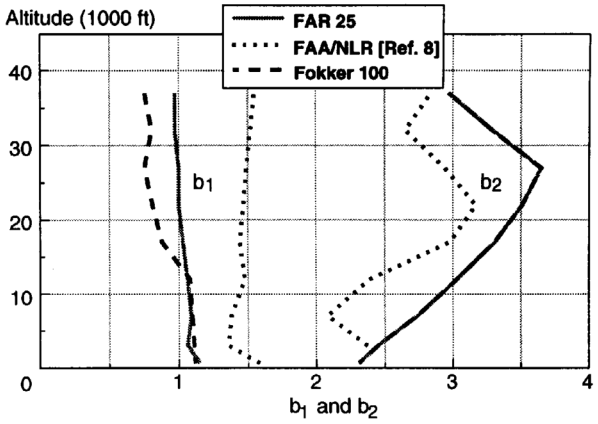

Fig. 8a Comparison of b_1 and b_2 values (m/s TAS)

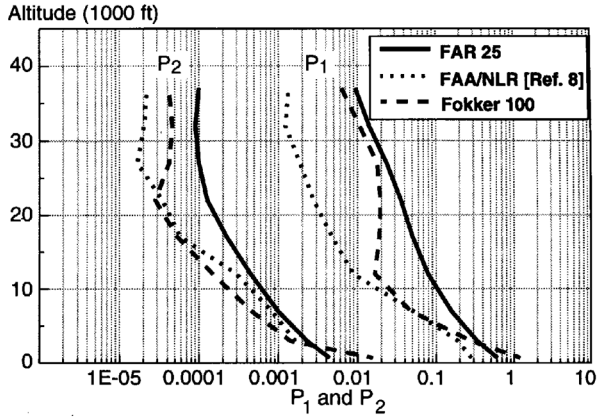

Fig. 8b Comparison of P_1 and P_2 values

Figure 8a shows the 'b'-values. The resulting b_1 for 'non-storm' conditions corresponds very well with the FAR/JAR-values, for lower altitudes. For altitudes above 15,000 ft the value for b_1 is smaller when compared to FAR/JAR data.
The 'storm'-parameter b_2 coincides (by choice) with the FAR/JAR-values.

Figure 8b presents the 'P'-values. Except for the lowest altitude bands, both P_1 and P_2 are smaller than FAR/JAR-values for all altitude bands.

The P_1-values have a tendency to follow the FAA/NLR results up to altitudes of ±10,000 ft. For higher altitudes the P_1-values approach the FAR-values again.
The P_2-values are smaller than FAR/JAR-values and follow the same trend as found from the FAA/NLR-results. From approximately 20,000 ft and higher the Fokker 100 results fall in between the FAR/JAR- and FAA/NLR-results.
It should be kept in mind however that the statistics from this analysis apply to one aircraft only, whereas the FAA/NLR results are obtained from a variety of different aircraft types.

The general conclusion is that at low altitudes more and at higher altitudes less turbulence is encountered than found from the FAR/JAR data. This can partly be explained by the fact that at higher (cruising) altitudes airplanes have the ability to avoid bad-weather conditions, contrary to lower altitudes where the airplanes usually have to follow ATC-directions, in combination with tight landing schedules and consequently hardly any choice in avoiding bad (turbulent/gusty) weather.

Discrete lateral gust

Since there is no formulation for instance from measurements that have been carried out in the past to obtain derived lateral-gust velocities, an approach has been used that is similar to the discrete vertical-gust approach. The derived gust velocity for lateral gust (U_{del}) is then found from:

$$U_{del} = \frac{(a_{yt})_{max}}{\bar{C}_{a_{yt}}} \qquad (19)$$

where a_{yt} is the lateral acceleration of the tail of the aircraft and $\bar{C}_{a_{yt}}$ is the corresponding response factor, which is defined by the maximum response due to a (1 - cosine) lateral gust with a length of 25 tail-chords. The lateral acceleration itself is defined by:

$$a_{yt} = (a_y)_{cg} - l_t.\dot{r} = (\ddot{h}_y + V.r) - l_t.\dot{r} \qquad (20)$$

where l_t is the distance between the centre of gravity and the location of the lateral accelerometer.
Because the parameters that determine the value of $\bar{C}_{a_{yt}}$ are not readily available in the data-base (e.g. yaw-rate or yaw acceleration) $\bar{C}_{a_{yt}}$ has been determined by using a table-look-up and interpolation procedure. To this purpose a dynamic response model has been used based on the aircraft's stability and control derivatives which has been applied to a number of conditions with varying altitude and airspeed. At zero altitude also different flap positions have been considered. For all cases an average weight, moment of inertia and cg-position has been assumed. The dynamic model was composed of two anti-symmetric rigid degrees of freedom (sideways motion and yaw).

In figure 9a-c derived gust velocities for both vertical and lateral gust are presented for the same three altitude bands that have been used in the previous graphs. It is observed that the U_{de}-values for lateral gust (U_{del}) are much higher than for vertical gust (± factor 2)!
This means that to calculate a lateral acceleration (design) level that would be comparable to the vertical acceleration level of a given U_{de}-value, a much larger U_{de} would have to be used for the lateral case, or reversibly, if one would apply the same level of U_{de} for both vertical and lateral cases, the lateral acceleration would be much too small!!
Hence U_{del} is not a good design parameter !

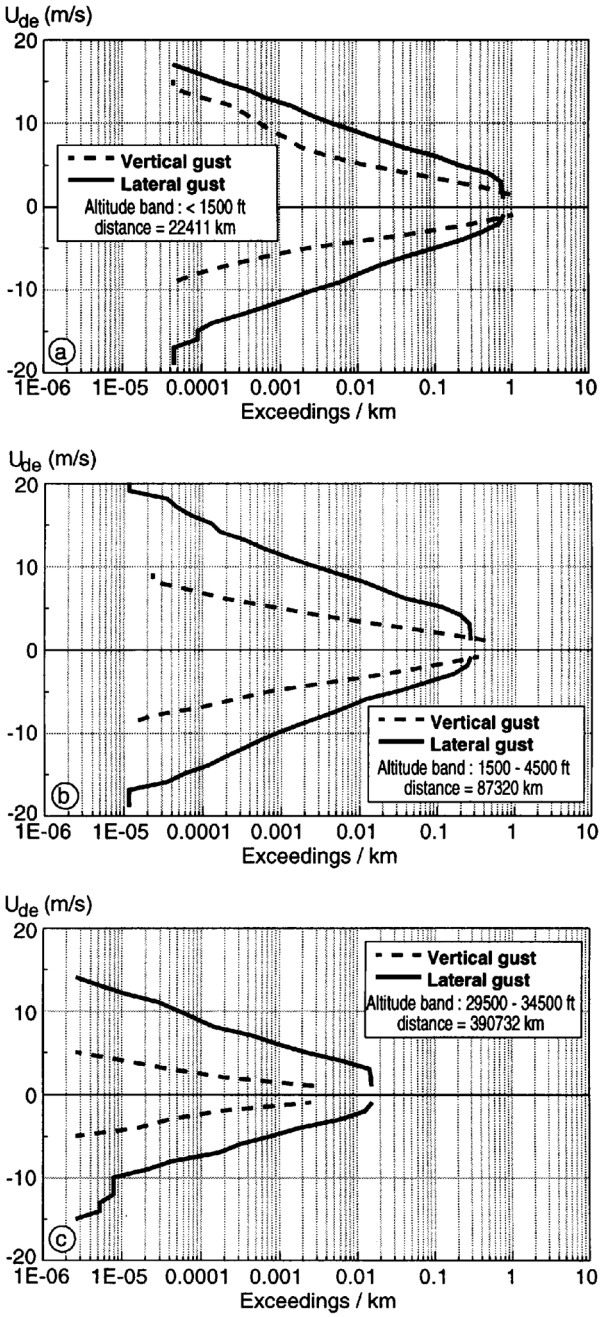

Fig. 9 Comparison of lateral & vertical U_{de}

Continuous lateral gust

Similar to the derived gust velocity for continuous vertical gust (U_σ), the derived gust velocity for lateral gust ($U_{\sigma l}$) can be found from:

$$U_{\sigma l} = \frac{a_{yt}}{\bar{A}} \qquad (21)$$

For the determination of vertical gust statistics in terms of U_σ use has been made of $(A)_{\Delta nz}$-values that could be obtained via the so-called "Houbolt" formula, valid for symmetric motions (pitch and heave). For asymmetric motions no such formula is available. Hoblit[13] provides in his book some figures and tables that can be used to estimate $\bar{A}$ for asymmetric motions, for instance $(\bar{A})_r$. Another possibility is to calculate and tabulate $A_{a_{yt}}$ in the same way as done in the previous section for $C_{a_{yt}}$.

Now $U_{\sigma l}$ is found from the peak accelerations of the lateral accelerometer mounted in the rear fuselage, following the 'peak-between-means' criterion.
To find the number of exceedances of $U_{\sigma l}$, one single lateral acceleration peak 'produces' $N(0)_{ref}/N(0)$ occurrences of lateral gust with intensity $U_{\sigma l}$.
Due to lack of an approximate method to estimate N(0) similar to equation 13, N(0) has been estimated based on the ratio of natural frequencies of the aircrafts pitch and yaw-modes according to:

$$\left[N(0)_{ref}\right]_{lat} = \left(\frac{f_{yaw}}{f_{pitch}}\right) \cdot \left[N(0)_{ref}\right]_{vert} \qquad (22)$$

The resulting exceedance data for the calculated $U_{\sigma l}$ are compared to U_σ-values as derived for vertical gust and plotted in figure 10a-c for three different altitude bands.
Taking into account that most (acceleration) exceedances occur at altitudes below 10,000 ft (67 %), a remarkable correspondence between the vertical and lateral results is observed in figures 10a and 10b, although U_σ for vertical gust is not symmetric and contains higher positive levels due to (pitching) manoeuvres. Lateral manoeuvring has a more symmetric character. Furthermore it is found from the measurements that the influence of lateral manoeuvring at higher altitudes is rather limited.
The higher altitude band (Fig. 10c) shows also a good correspondence between lateral and vertical derived U_σ's.
Despite the fact that the statistics for both vertical and lateral gust may contain manoeuvring effects, the correspondence between the vertical and lateral gust statistics is an indication that the atmosphere is isotropic, at least for these two perpendicular directions.

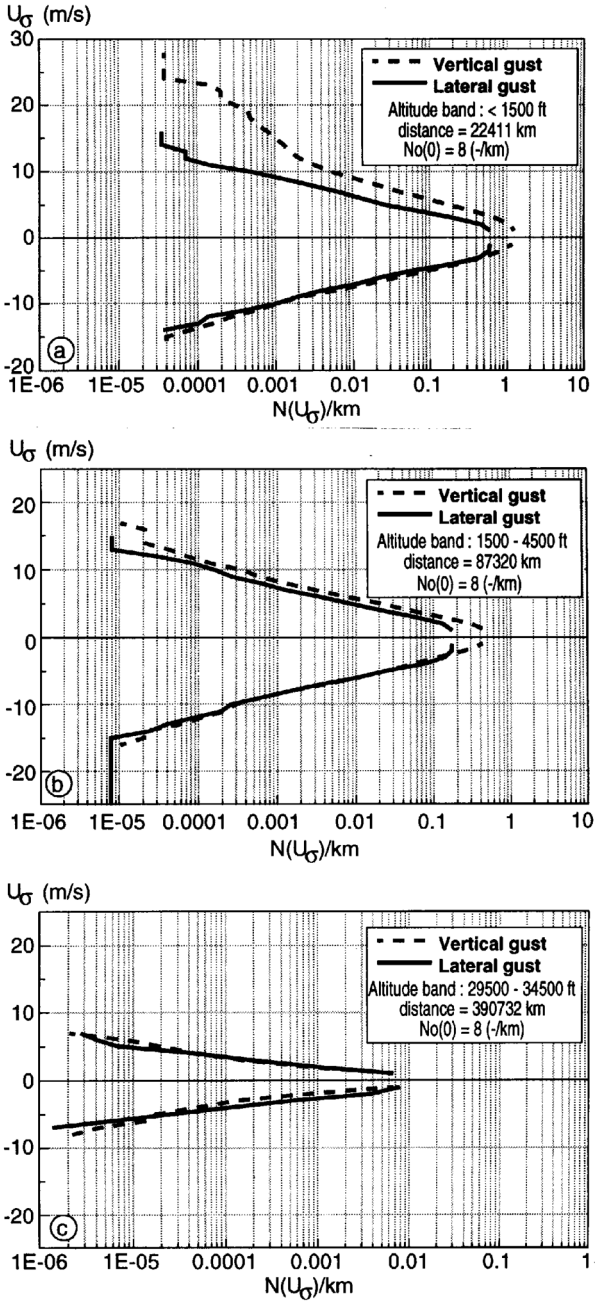

Fig. 10 Comparison of vertical & lateral U_σ's

Conclusions

- A description is given of the measurements of vertical and lateral accelerations of a commercially operated Fokker 100 aircraft.
- Although the database with ±2000 flights is rather small compared to the vast amount of flights in the databases used in the FAA/NLR study[7] the information is considered to be relevant especially for 'non-storm' conditions.
- Comparison of vertical and lateral derived gust (U_{de}) showed that the discrete (1-cosine) approach will yield wrong (too small) acceleration-values, when for lateral gust the same velocities are applied as for vertical cases.
- Comparison of continuous (PSD) gust statistics showed that lateral and vertical U_σ-exceedance curves are comparable indicating that turbulence has (at least for these two perpendicular directions) an isotropic character.

Acknowledgement

The investigations described in this paper have been carried out under contract with the Netherlands Agency for Aerospace Programs (NIVR) in cooperation with (the former) Fokker Aircraft BV and KLM Royal Dutch Airlines.

References

1 K.G. Pratt, W.G. Walker, "A revised gust load formula and a re-evaluation on VG data taken on civil transport airplanes from 1933 to 1950", NASA Report 1206, 1964.
2 C.G. Peckham, "A Summary of Atmospheric Turbulence Recorded by NATO Aircraft", AGARD Report No. 586, 1971.
3 I.W. Kaynes, "A summary of the Analysis of Gust Loads Recorded by Counting Accelerometers on Seventeen Types of Aircraft", AGARD Report No. 605.
4 B.W. Payne, A.E. Dudham, K.C. Griffith, "Re-assessment of Gust Statistics using CAADRP Data", AGARD Report No. 738, 1986.
5 J.B. de Jonge, "Acquisition of statistical gust load data by commercial airplanes", AGARD AG-317, May 1991.
6 J.B. de Jonge, "Reduction of Δn_z acceleration data to gust statistics", NLR CR 92003 L, January 1992.
7 J.B. de Jonge, P.A. Hol, P.A. van Gelder, "Re-Analysis of European flight loads data", NLR TP 93535, November 1993, Revised Edition February 1996, also published as DOT/FAA/CT-94/21 May 1994.
8 P.A. van Gelder, "Acquiring Tail Load Spectra from In-Flight Measurements", AIAA 93-1607, (also published as NLR TP 93020).
9 P.A. van Gelder, "In-Flight Tail Load Measurements", ICAS-92-6.5.2, (also published as NLR TP 92158).
10 P.A. van Gelder, "Analysis of measured in-flight tail loads", ICAS-96-5.3.2, (also published as NLR TP 96279).
11 T.J. Barnes, T. DeFiore, "The new FAA Flight Loads Monitoring Program", AIAA 91-0258, 1991.
12 "Flight Loads Data for a Boeing 737-400 in Commercial Operation", DOT/FAA/AR-95/21, April 1996.
13 F.M. Hoblit, "Gust Loads on Aircraft: Concepts and Applications", AIAA Education series, ISBN 0-930403-45-2, 1988.
14 J.C. Houbolt, "Status review of atmospheric turbulence and aircraft response", in AGARD report No. 734, december 1987, ISBN 92-835-0426-7.
15 G. Coupry, "Improved reduction of gust loads data for gust intensity", in AGARD-AG-317, May 1991, ISBN 92-835-0617-0.

Abbreviations

ACMS	Aircraft Condition Monitoring System
ATC	Air Traffic Control
CAA	Civil Aviation Authority
CAADRP	CAA Data Reduction Programme
FAA	Federal Aviation Administration
FAR	Federal Aviation Regulation
JAA	Joint Aviation Authorities
JAR	Joint Aviation Requirements
KLM	Koninklijke Luchtvaart Maatschappij (Royal Dutch Airlines)
KSSU	KLM, SAS, Swissair, UTA - aircraft maintenance combination
NACA	National Advisory Committee for Aeronautics
NLR	Nationaal Lucht- en Ruimtevaart-Laboratorium (National Aerospace Laboratory)
ONERA	Office National d'Études et de Recherches Aérospatiales
PSD	Power Spectral Density
RAE	Royal Aircraft Establishment